

Supporting Information

A turn-on optoacoustic probe for imaging metformin-induced upregulation of hepatic hydrogen sulfide and subsequent liver injury

Lihe Sun, Yinglong Wu, Junjie Chen, Jun Zhong, Fang Zeng* and Shuizhu Wu*

State Key Laboratory of Luminescent Materials & Devices, College of Materials Science & Engineering, South China University of Technology, Guangzhou 510640, China.

*Authors to whom correspondence should be addressed:

Fang Zeng, Email: mcfzeng@scut.edu.cn

Shuizhu Wu, Email: shzhwu@scut.edu.cn

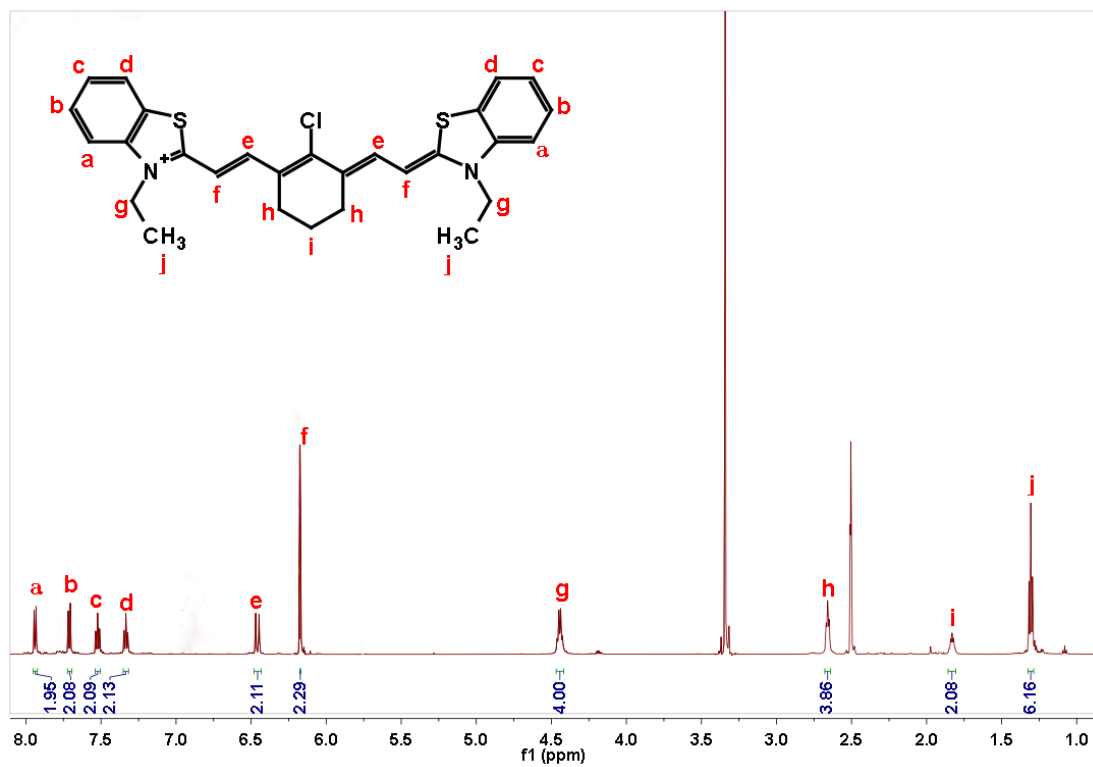


Figure S1. ¹H NMR spectrum of Compound 2.

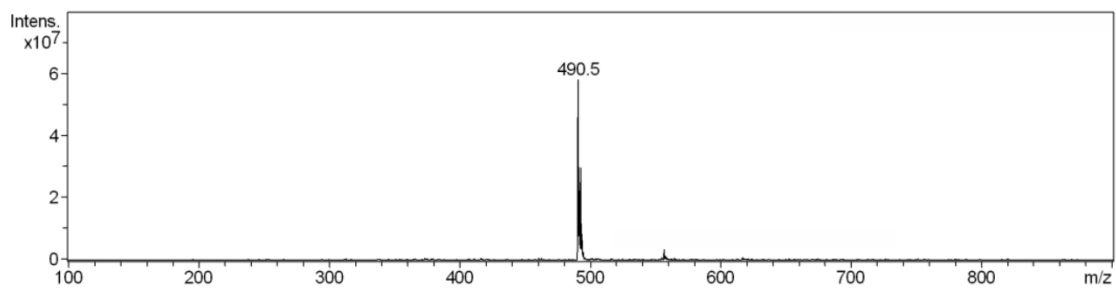


Figure S2. Mass spectrum of Compound 2. m/z 490.5 [M]⁺.

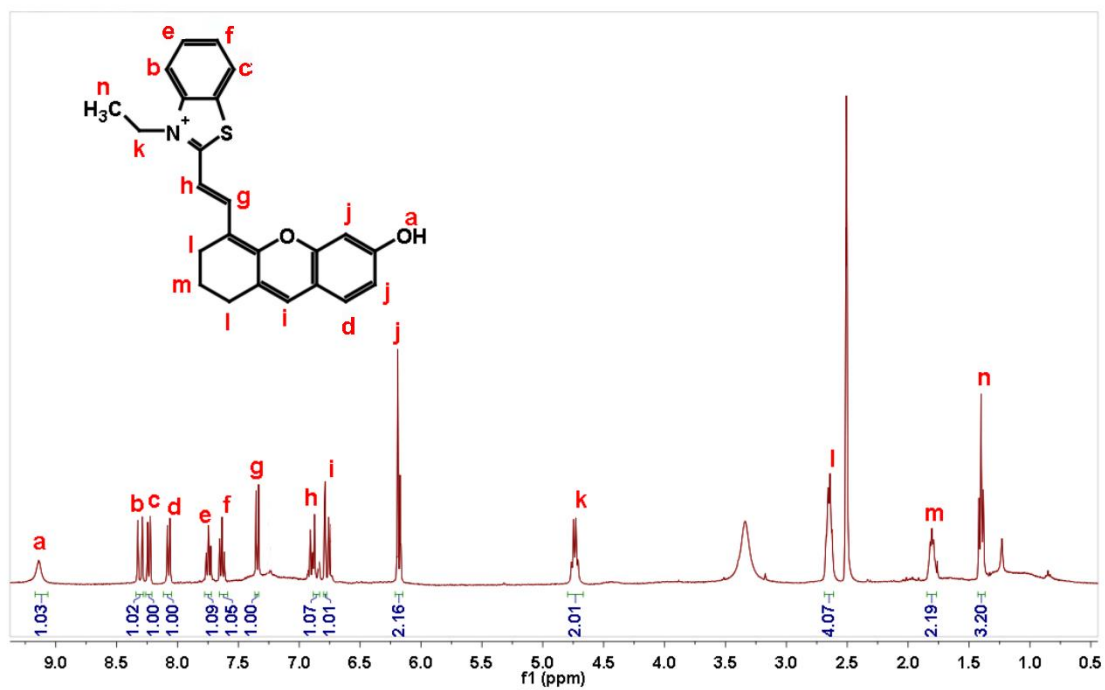


Figure S3. ¹H NMR spectrum of Compound 3.

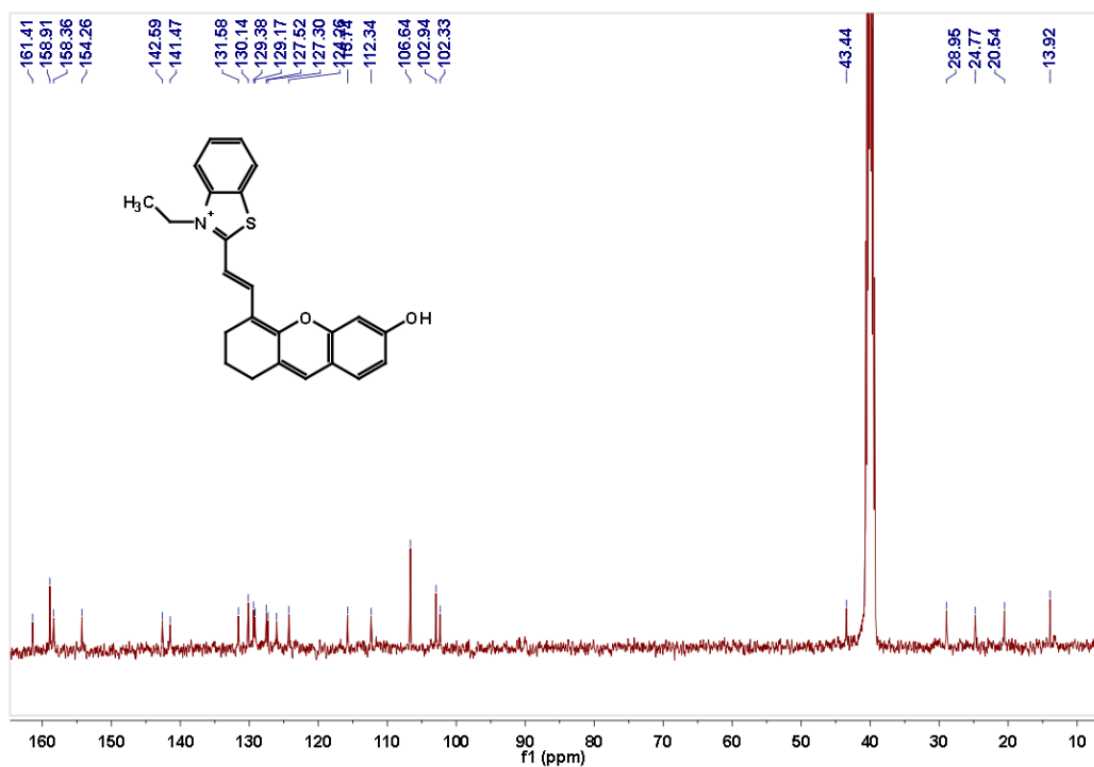


Figure S4. ¹³C NMR spectrum of Compound 3.

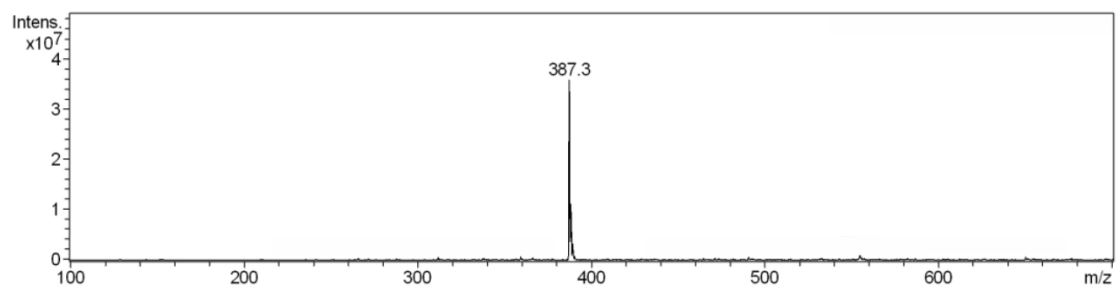


Figure S5. Mass spectrum of Compound 3. m/z 387.3 $[M]^+$.

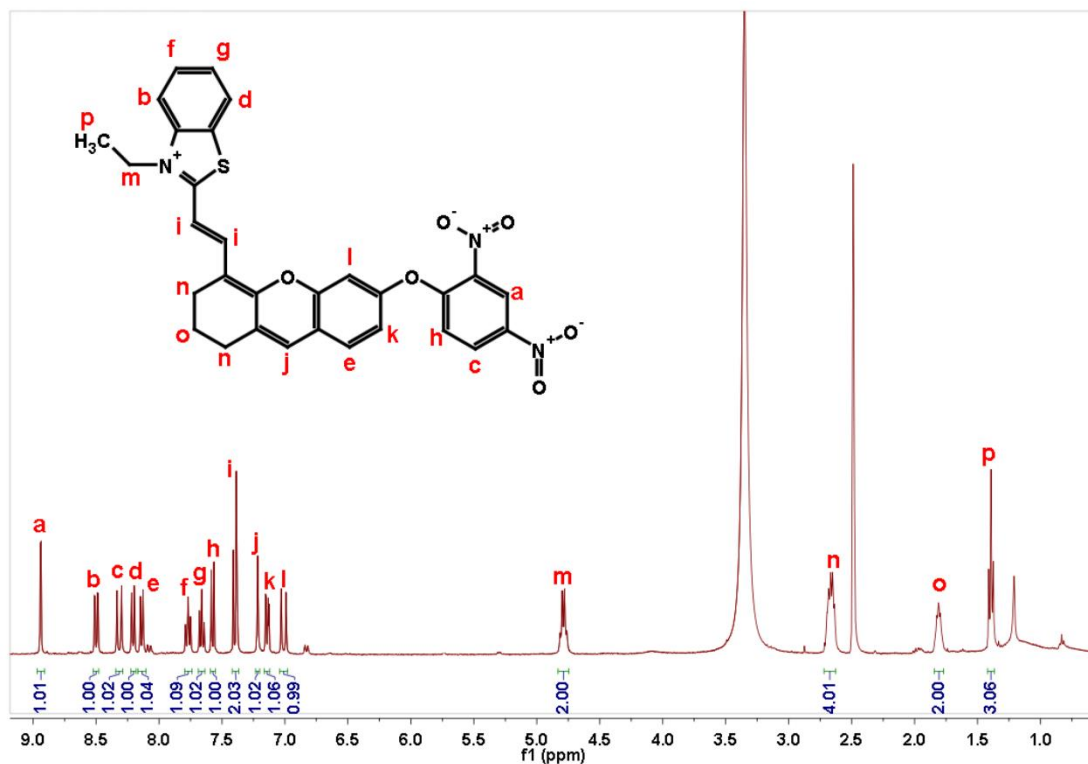


Figure S6. ^1H NMR spectrum of Compound 4.

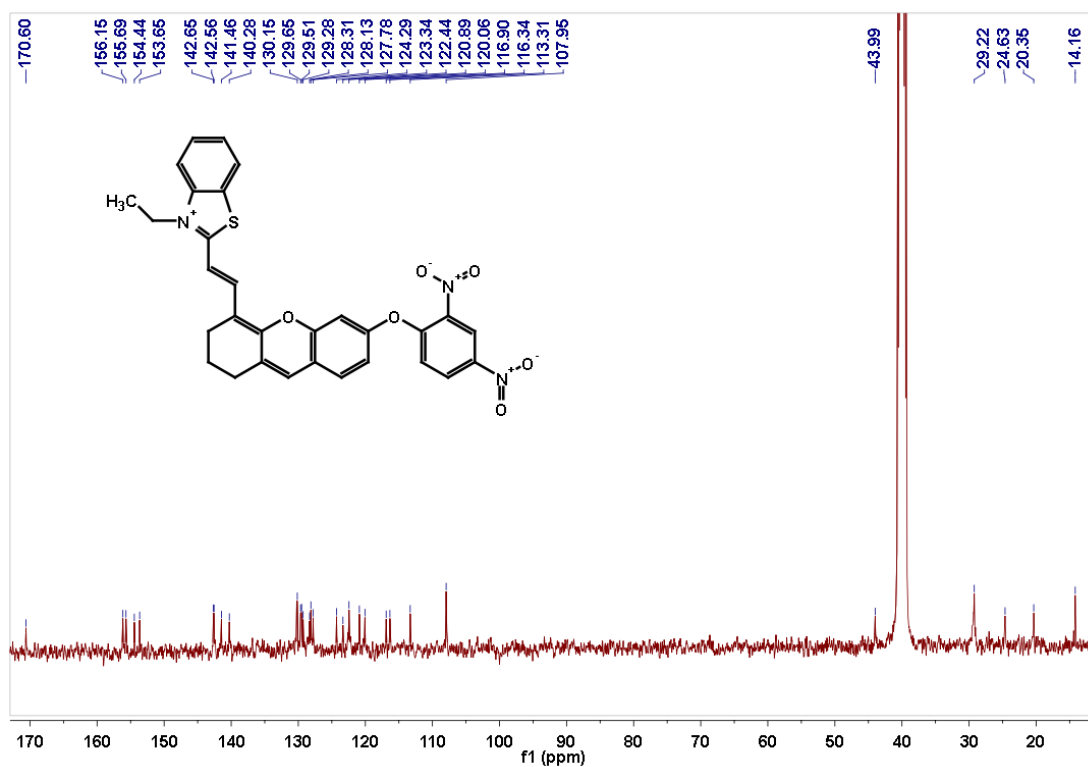


Figure S7. ^{13}C NMR spectrum of Compound 4.

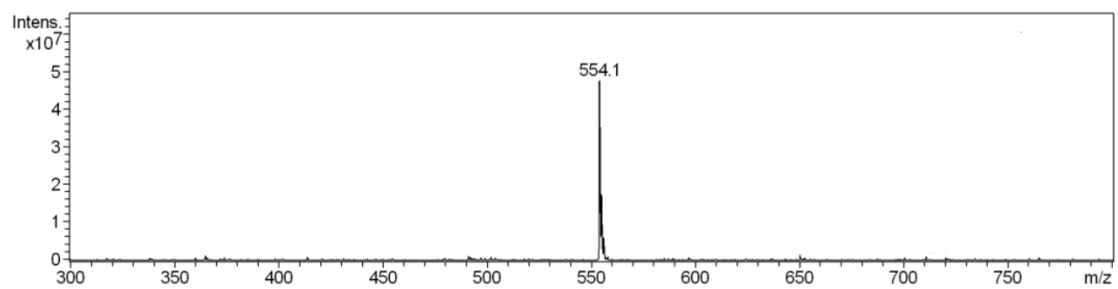


Figure S8. Mass spectrum of Compound 4. m/z 554.1 $[M]^+$.

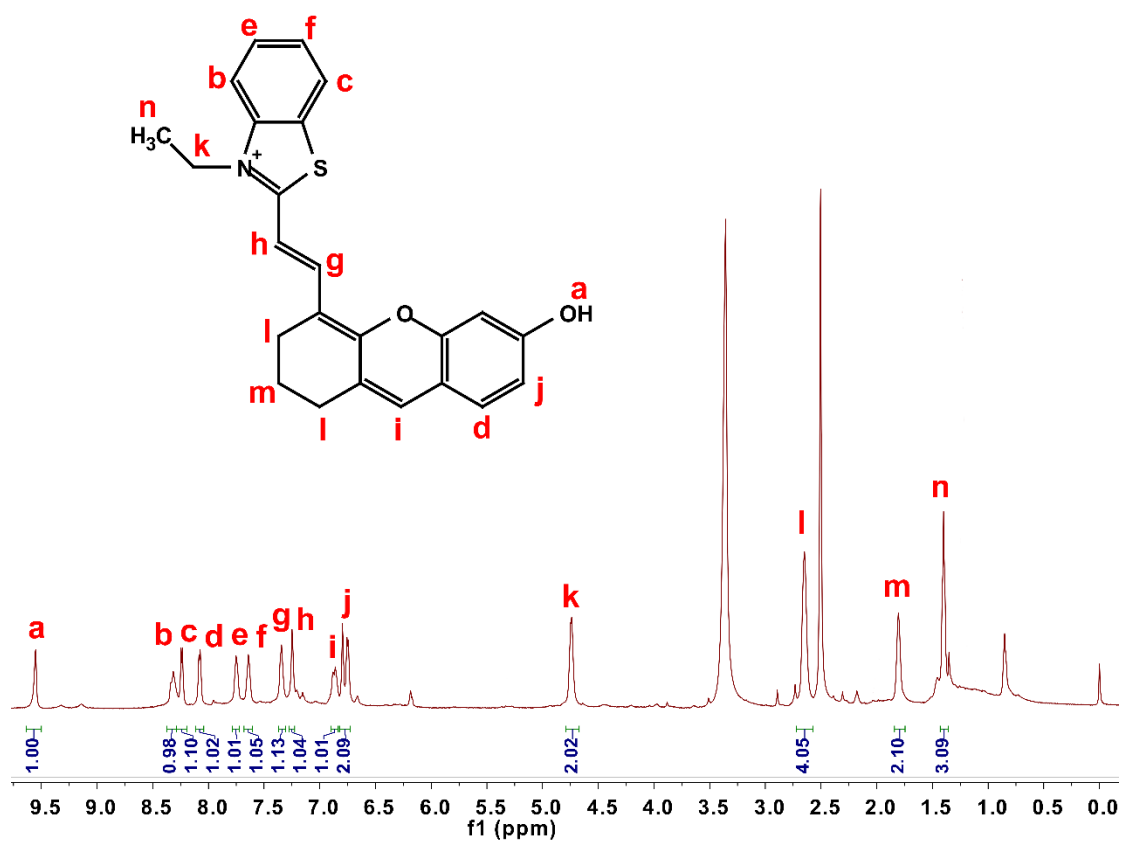


Figure S9. ¹H NMR spectrum of the product from the reaction of NR-NO₂ and NaHS. (which was purified by silica gel column chromatography).

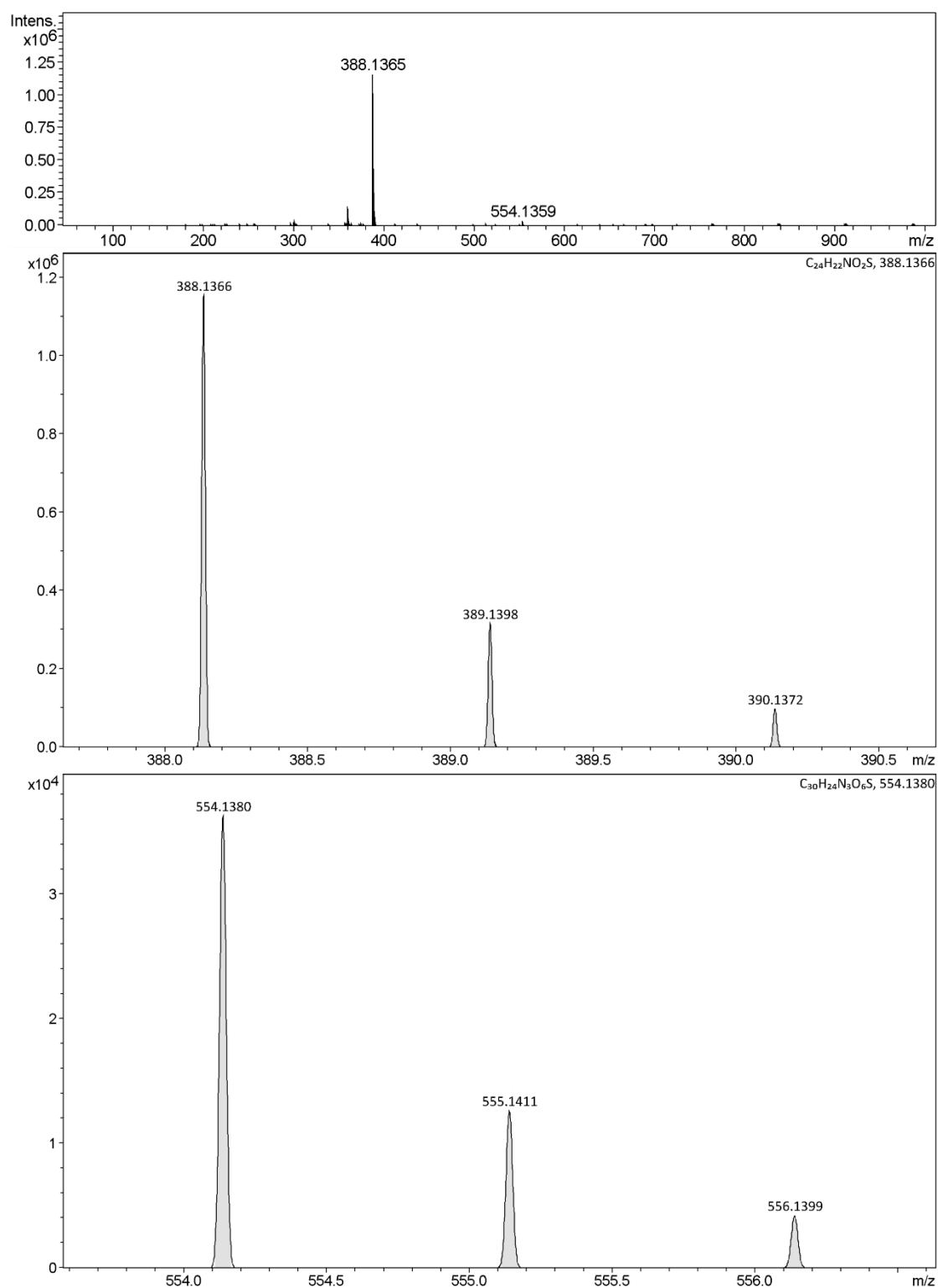


Figure S10. HR-MS spectra. A solution of NR-NO₂ in methanol added with NaHS was used for the measurement. Top row: full spectrum scan, NR-NO₂ [M]⁺ m/z 554.13 and NR-OH [M+H]⁺ m/z 388.13. Middle row: partial enlargement of the spectrum focusing on NR-OH [M+H]⁺. Bottom row: partial enlargement of the spectrum focusing on NR-NO₂ [M]⁺.

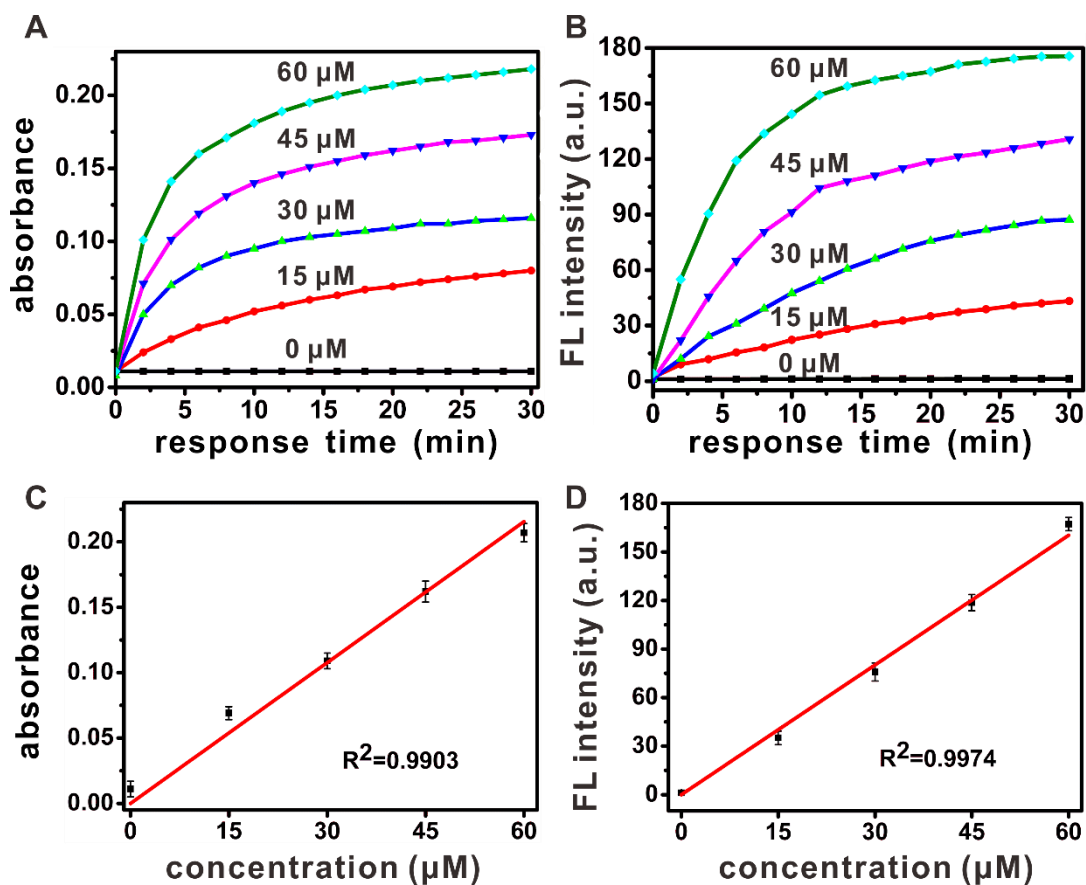


Figure S11. (A) Absorbance of the probe at 695 nm upon treatment of different concentrations of NaHS for different time. (B) Fluorescent intensity of the probe at 725 nm upon treatment of different concentrations of NaHS for different time. (C) Absorbance of the probe at 695 nm after 20 min incubation with different concentrations of NaHS. (D) Fluorescent intensity of the probe at 725 nm after 20 min incubation with different concentrations of NaHS.

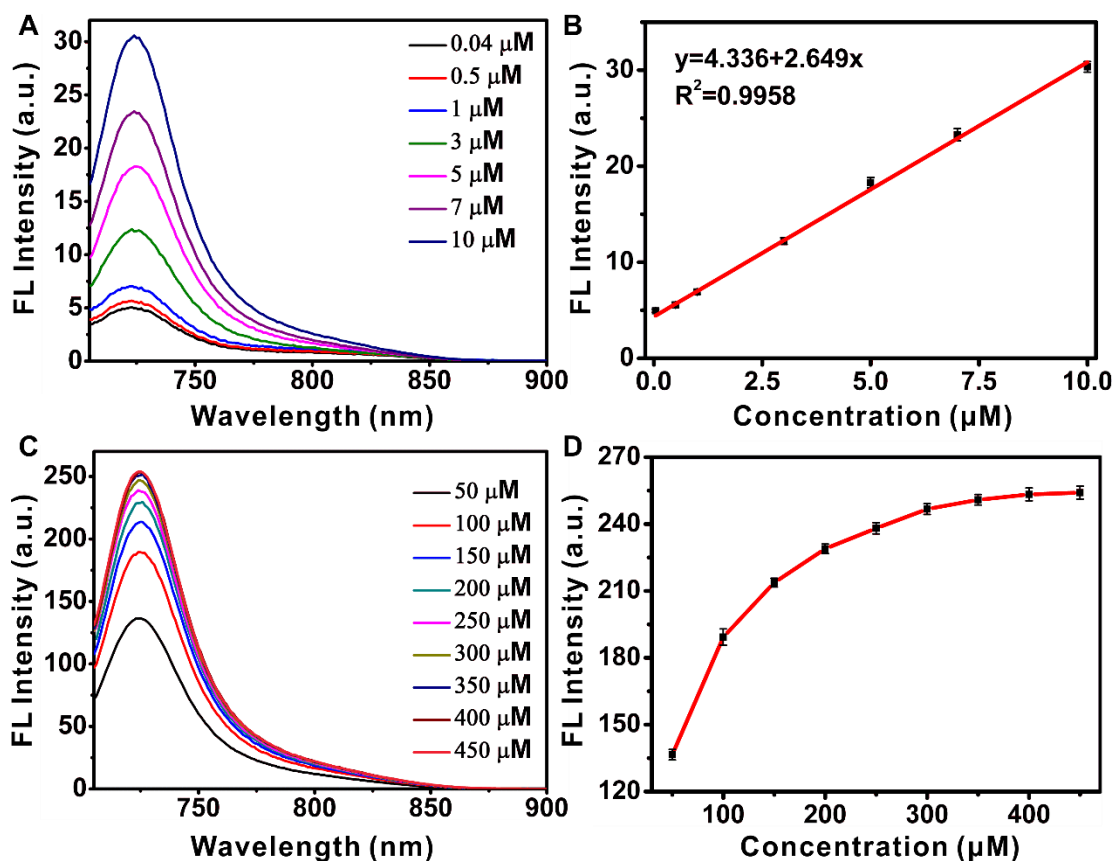


Figure S12. (A) Fluorescence spectra of NR-NO₂ after incubation with different concentrations of NaHS. (B) Fluorescent intensity at 725 nm after incubation with different concentrations of NaHS (0.04, 0.5, 1, 3, 5, 7 and 10 μM). (C) Fluorescence spectra of NR-NO₂ after incubation with different concentrations of NaHS. (D) Fluorescent intensity at 725 nm after incubation with different concentrations of NaHS (50, 100, 150, 200, 250, 300, 350, 400 and 450 μM).

The method for determining the limit of detection (LOD):

First the calibration curve was obtained from the plot of fluorescent intensity at 725nm (I_{725}) versus NaHS concentrations. The regression curve equation was then obtained for the lower concentration part.

$$\text{LOD} = 3 \times \text{S.D.} / k$$

Where k is the slope of the curve equation, and S.D. represents the standard deviation for I_{725} in the absence of NaHS.

$$I_{725} = 4.336 + 2.649 \times [\text{NaHS}] \quad (R^2 = 0.9958)$$

$$\text{LOD} = 3 \times 0.0353 / 2.649 = 0.04 \mu\text{M} = 40 \text{ nM}$$

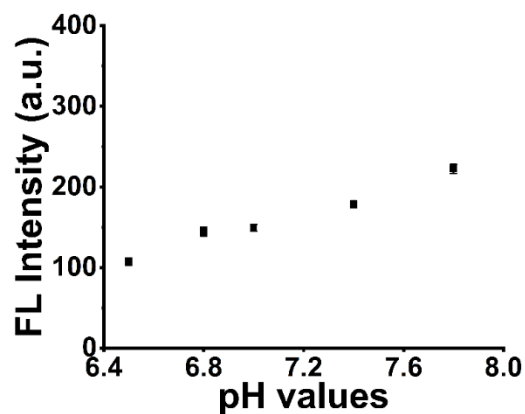


Figure S13. Fluorescent intensity of the probe at 725 nm after incubation with NaHS (60 μ M) at different pH environment.

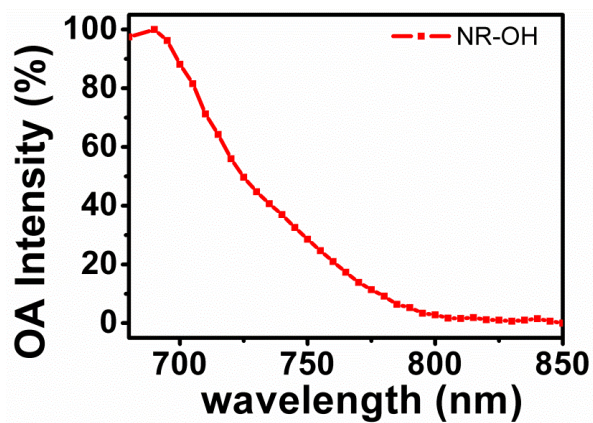


Figure S14. Optoacoustic intensities (%) of NR-OH at different wavelengths.

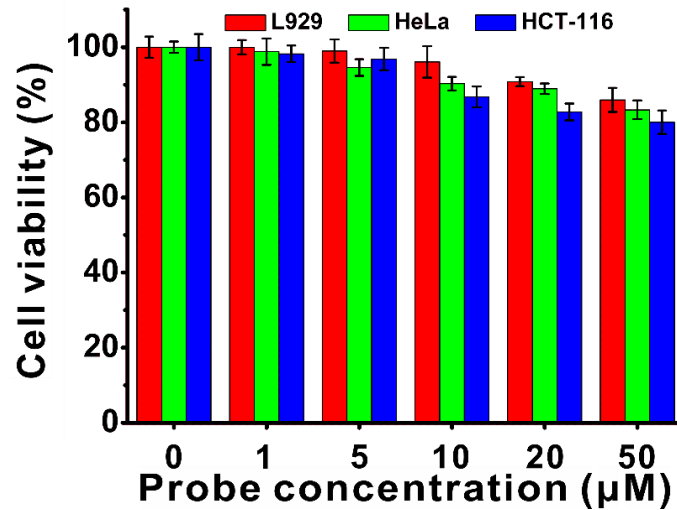


Figure S15. Viabilities of L929, HeLa and HCT-116 cells after 24 h of incubation with different concentrations of the probe (0, 1, 5, 10, 20 and 50 µM).

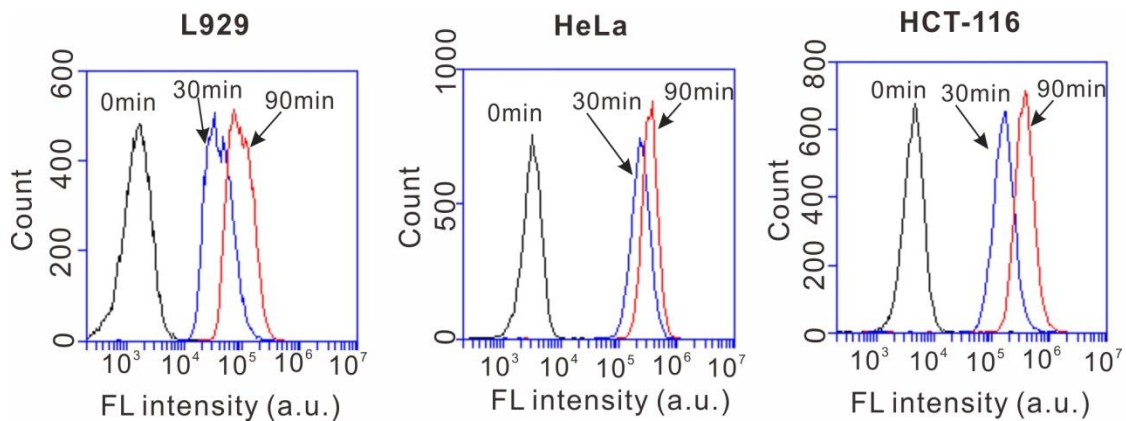


Figure S16. Cellular uptake of NR-NO₂ evaluated by flow cytometry analysis (cell counts: 10,000; probe concentration: 30 µM; incubation time: 0, 30 and 90 min).

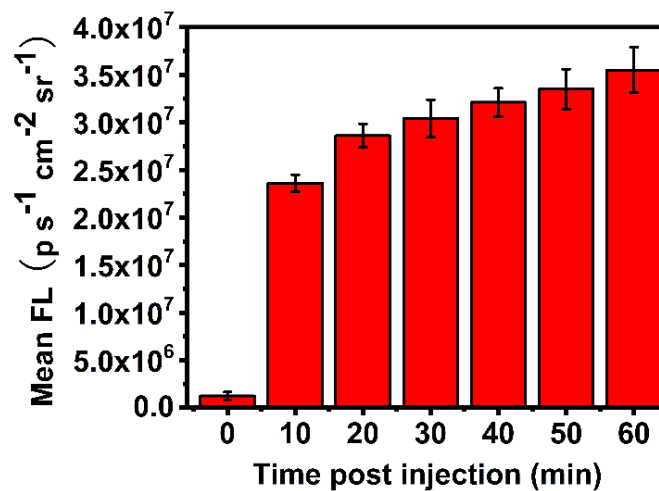


Figure S17. Mean fluorescence intensities in ROI of the tumor-bearing mice at different time after intratumoral injection of the probe (n=6).

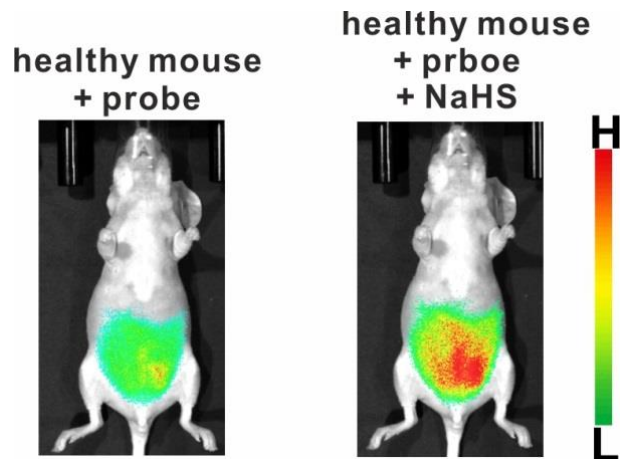


Figure S18. In vivo fluorescence images of NR-NO₂ (i.p. injection) towards H₂S (endogenous and exogenous) in mice with different treatment.

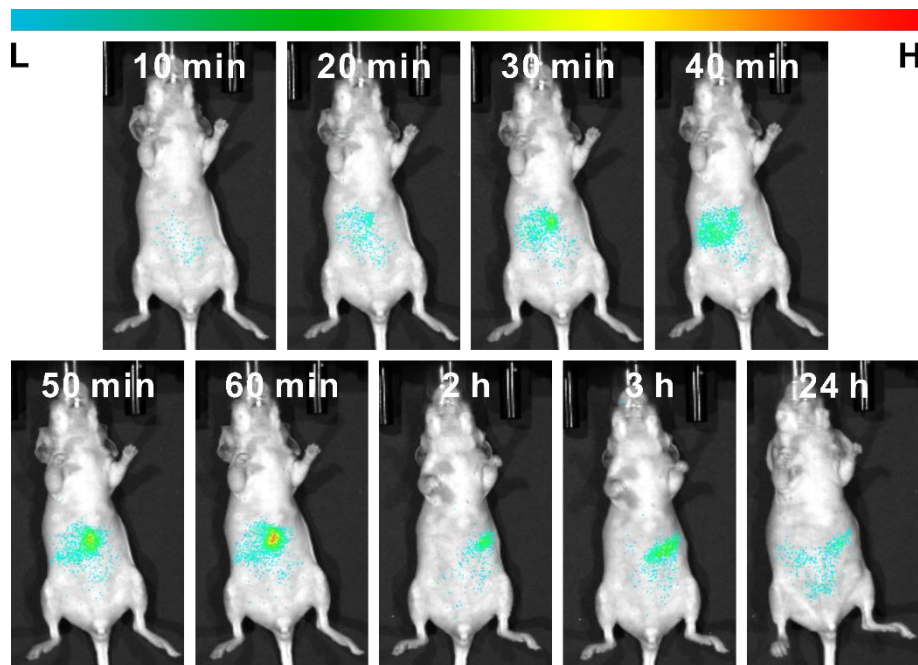


Figure S19. In vivo fluorescence images of 1 mg metformin-treated mice at different time after i.v. injection of NR-NO₂ through tail vein.

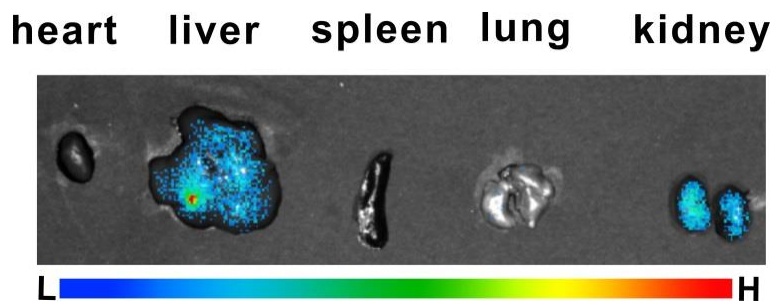


Figure S20. Fluorescence images of isolated organs from 1 mg metformin-treated mice by using Ami imaging system (the mice were euthanized and dissected at 60 min after i.v. injection of NR-NO₂).

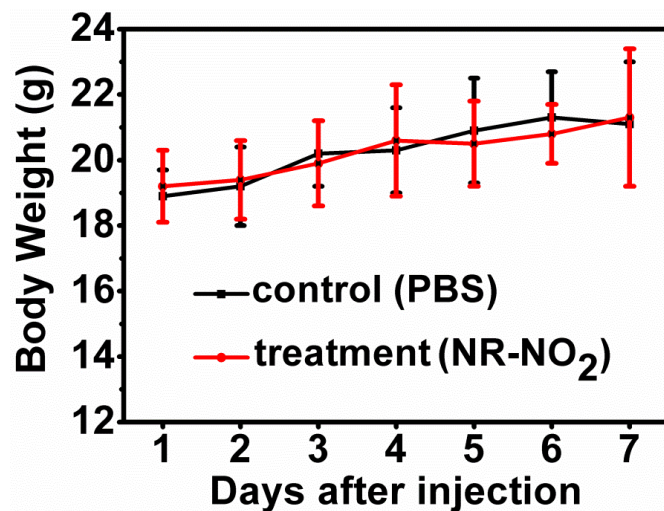


Figure S21. Mice body weight within one week after i.v. injection of PBS or probe solution (2.8 mg probe/kg body weight, in PBS containing 2% DMSO).

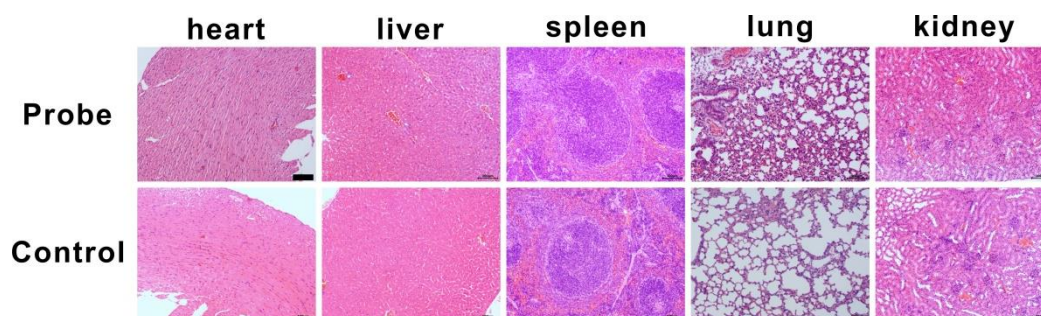
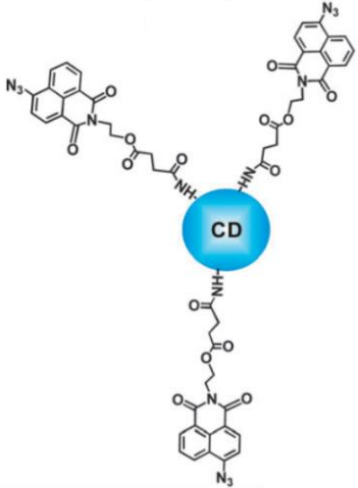
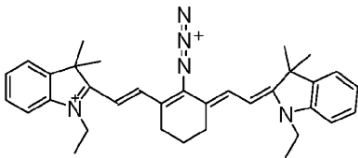
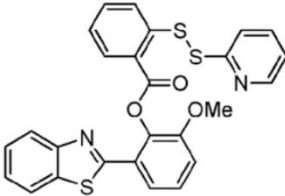
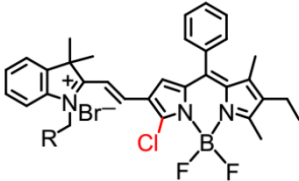
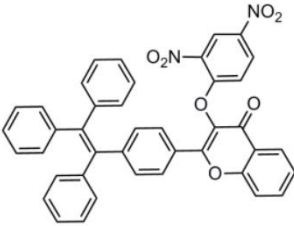
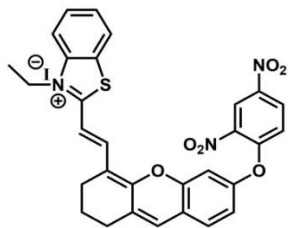


Figure S22. Representative histological sections (H&E staining) of heart, liver, spleen, lung and kidney from the control group and the mice group pretreated with NR-NO₂ (scale bar: 100 μm).

Table S1. Comparison of the reported fluorescent and optoacoustic probes for H₂S imaging and corresponding limit of detections (LOD).

Probes (fluorescent or optoacoustic)	LOD
 <p data-bbox="328 893 1118 927">Fluorescent probe. Chem Commun (Camb). 2013; 49: 403-5.</p>	10 nM
 <p data-bbox="320 1122 1126 1155">Fluorescent probe. Chem Commun (Camb). 2012; 48: 2852-4.</p>	80 nM
 <p data-bbox="312 1391 1134 1424">Fluorescent probe. Chem Commun (Camb). 2012; 48: 10871-3.</p>	120 nM
 <p data-bbox="405 1662 1043 1695">Photoacoustic probe. Chem Sci. 2017; 8: 2150-5.</p>	53 nM
 <p data-bbox="363 1975 1085 2009">Fluorescent probe. Mater Chem Front. 2017; 1: 838-45.</p>	90 nM



Optoacoustic and fluorescent probe. NR-NO₂ (this work)

40 nM